



## UTILIZATION OF WASTE FOIL AND CARBIDE SLAG AS HETEROGENEOUS CATALYST FOR *IN-SITU* TRANSESTERIFICATION OF *Ricinus Communis* (CASTOR SEEDS)

<sup>1</sup>Muhammad Ahmad Galadima, <sup>1</sup>Musa Usman Dabai, <sup>2</sup>Bilyaminu Rafi Ahmad, <sup>3</sup>Jamilu Ibrahim Umar

<sup>1</sup>Department of Pure & Applied Chemistry, Usmanu Danfodiyo University, Sokoto

<sup>2</sup>Department of Chemistry Nigeria Army University Biu, Borno.

<sup>3</sup>Shehu Shagari College of Education, Sokoto

\*Corresponding authors' email: [ahmadgldm@gmail.com](mailto:ahmadgldm@gmail.com) Phone: +2348162299623

### ABSTRACT

Contemporary studies on exploration of waste to eco-friendly approach of biodiesel catalysis have attracted much attention. This study produce a heterogeneous catalysts with high activity from Carbide slag and waste Aluminum foil digested in Conc.  $\text{HCl}_{(\text{aq})}$  calcined at high temperatures. The produced catalyst applied in *In-situ* transesterification with castor bean seed possess enormous potential towards developing an economical and ecological sound biodiesel generation. The catalyst was characterized using FT-IR, SEM and X-ray diffraction (XRD), methods. Optimization of the reaction variables was carried out using respond Surface Methodology (RSM) Box-Behnken experimental designs. The empirical model obtained expresses the relationship between the biodiesel and the statistical significant reaction variables ( $R^2 = 90.15\%$ ). The conversion of 97.68% was achieved under the optimum reaction conditions of 1.5g. wt of  $\text{CS-AlCl}_3_{(\text{aq})}$ , (1:9) of seed to methanol ratio, 1hrs of reaction time and  $40^\circ\text{C}$  of temperature. The biodiesel produced were characterized using FTIR and GC-MS. The study is an earliest effort to generate low-cost, eco-friendly, effective and reusable catalyst from waste aluminium foil and carbide slag for biodiesel production.

**Keywords:** *Ricinus Communis*, Biodiesel, In-situ transesterification, optimization, Box-Behnken

### INTRODUCTION

Consistent hike in universal energy usage, the biomass-to-fuel processes are increasingly becoming important areas to the energy industry and policy makers throughout the world. Biodiesel production is taking steps in restoring the heavy dependence over fossil fuels. Owing to its various advantages, the global consumption of biodiesel had expand from 0.25 billion gallons in 2006 to 2.0 billion gallons in 2018, and the trend of biodiesel expansion has also been projected to be linear in the future years (Galadima and Muraza, 2020). Meanwhile the *In-situ* transesterification is one of the attractive and cost effective methods for producing biodiesel with the elimination of pre-separation steps. *In-situ* transesterification (ISTE) method reduces the production cost of biodiesel and produced greater yield than the conventional method (Samuel *et al.*, 2012). The recent interest in biodiesel indicated a shift to industrial wastes as another approach for escalating greener industrial process and eco-scientific efficiencies. *Ricinus communis* (castor bean) is a high prospective feedstock, which could supply up to 60% of the non-edible oil needed to produce biodiesel. The main fatty acid in castor oil is ricinoleic acid ( $\text{C}_{18}\text{H}_{34}\text{O}_3$ ), with approximately 85-90% of total fatty acid content. It gives characteristics such as high viscosity, high miscibility, low iodine content, low freezing point, which make it an appropriate raw material to produce biodiesel (Bauddh *et al.*, 2015; Mckee, 2016). In this perspective, this study focuses on the synthesis of biodiesel via *In-situ* transesterification utilizing wastes foil and carbide slag as an economical and greener catalyst in transesterification of non-edible seed oil into biodiesel which can serve as potential future prospects for competitive biodiesel.

### MATERIALS AND METHODS

#### Sample Collection and Preparation

*Ricinus communis* (Castor bean) were cultivated in Dabagi farm, 33kilometer along Sokoto-Gusau road, North-western

Nigeria. The seeds were decorticated and stored at room temperature for one week and subsequently dried in the oven at  $105^\circ\text{C}$  to remove the remaining moisture until a constant weight was achieved. The carbide slag was obtained in Kanti daji Marmarun Nufawa, Sokoto, Nigeria at coordinates:  $13^\circ03'25.4''\text{N}$   $5^\circ13'10.8''\text{E}$ . While waste aluminium foil were collected from several Chicken frying sports centres in Sokoto metropolis while Methanol (99.8% purity), n-Hexane and Hydrochloric acid (36% purity) were purchased from a local chemical dealer.

#### Preparation of Catalysts

Waste aluminium foil (10.5g) was chopped to small pieces and digested in  $60\text{cm}^3$  of Conc.  $\text{HCl}_{(\text{aq})}$  to form concentrated solution. The solution was cooled and filtered using 150mm filter paper. Measure  $50\text{cm}^3$  from the concentrated solution was doped with carbide slag in a round bottom flask equipped with magnetic stirrer on a heating mantle at 700rpm at  $40^\circ\text{C}$  for 3hrs. After which the catalyst was dried using laboratory oven for 5hrs at  $105^\circ\text{C}$  for complete dryness. The prepared carbide slag/Aluminium foil solution denoted as  $(\text{CS-AlCl}_3_{(\text{aq})})$  was ground, sieved to obtain a particle size of 100 meshes. The obtained fine powder was then calcined using a muffle furnace at the temperature range of  $(400-1100^\circ\text{C})$  for 4hrs.

#### Characterization of Catalyst

The prepared catalyst was characterized using various Techniques. The FTIR spectra of the sample were analyzed at the Central Laboratory Complex (CASLaC), Usman Danfodiyo University Sokoto with FT-IR Carry 630 spectrometer using KBr pellet technique. The X-ray diffraction pattern of the catalyst was analyzed using Rigaku Miniflex EDXRF at the Central Laboratory Complex (CASLaC), The operating data used were at scan rate of  $5^\circ$

min<sup>-1</sup> and at 2θ range of 10-80° with a step size of 0.017°. The Cu Kα X-ray (λ= 0.154nm) was nickel filtered.

### Design of Experiment

Response Surface (Box-Behnken) Statistical Experimental Design was used for optimization. Four independent variables; reaction time, temperature, methanol-to-seed ratio and weight of catalyst (CS-AlCl<sub>3(aq)</sub>) were selected for the investigation, based on preliminary experiments conducted (Ehimen et al., 2010). Each trial was duplicated to obtain 54 completely randomized trials.

### Description of Experimental Runs

In each trial, milled palm kernel nuts (150.0g) was mixed with 60cm<sup>3</sup> of n-hexane as co-solvent for 10min; the slurry obtained was transferred into cellulose thimble with an appropriate volume of methanol (40, 45 or 60 cm<sup>3</sup>) to forge 1:9 of Seed to methanol mole ratio then mixed with 0.45, 0.92 or 1.5 g of the activated catalyst in a 250 cm<sup>3</sup> round bottomed flask equipped with a reflux condenser at temperatures of 40, 50 and 60°C under constant stirring at 600 rpm for specific period of 1, 2, or 3hrs. The products were transferred into a separating funnel and 10cm<sup>3</sup> of distilled water and 10cm<sup>3</sup> of n-hexane were added for 1hr, forming three phases (the upper layer of biodiesel, the middle layer of glycerol and the lower layer of the catalyst). The excess methanol was distilled off and the biodiesel was collected, washed with distilled water and dried over anhydrous sodium sulphate; the biodiesel thus obtained was finally oven-dried at 60°C and 60 minutes. The biodiesel yield was calculated relative to the weight of the oil in 50g of the seed (Eq. 1) (Muhammad et al., 2017).

#### Biodiesel yield

$$= \frac{\text{wt of biodiesel obtained (g)} \times 100}{\text{wt of crude oil in 100g sample (g)}} \quad 1$$

### Data Analysis

The biodiesel yields obtained from *in-situ* transesterification experiment were analyzed on MINITAB 17 Statistical Software to estimate the interaction outcome of the reaction variables ( $x_i$ ) on the biodiesel yield ( $y$ ). The percentage of biodiesel yield fit the full quadratic polynomial regression model using regression analysis (Eq.2). Where:  $\beta_0$ ,  $\beta_i$ ,  $\beta_{ii}$ ,  $\beta_{ij}$  are the intercept, linear, quadratic and interaction coefficients respectively. Analysis of Variance (ANOVA) at 95% confidence level, and fitness of the model was measured from the coefficient of determination ( $R^2$ ). Contour graphs were plotted based on the fitted quadratic polynomial equation obtained from regression analysis, holding two of independent variables (reaction time, temperature, methanol and weight of catalyst) at a constant value while changing the other variables.

$$y = \beta_0 + \sum_{i=1}^4 \beta_i x_i + \sum_{i=1}^4 \beta_{ii} x_i^2 + \sum_{i=1}^4 \sum_{j=i+1}^4 \beta_{ij} x_i x_j \quad 2$$

### Biodiesel Assay

The biodiesel produced were analyzed using GC/MS Agilent 6890N GC coupled to Agilent 5973MSD. Total ion current (TIC) procedure was used. The solvent cut for all the fractions obtained took 5 minutes. Helium was used as the carrier gas at a flow rate of 1.2cm<sup>3</sup>/minutes. One micro litre (1µl) of the

samples was injected into injection port of the Gas chromatography machine at injection temperature of 250°C; the machine was equipped with 30m long polysilohexane capillary column with 20µm internal diameter and 1.0µ film thickness. The column oven temperature was programmed between 50-300°C at 5°C/minute and held at the final temperature for 10minutes (Tarigan et al., 2017). The compounds were identified using their respective mass spectra in comparison with standard mass spectra in NISTII Reference Library (Watto et al., 2015). The peaks of individual methyl esters were identified by comparing the retention time of each component in the reaction samples with the peaks of pure methyl ester standard compound. The concentration (C) of FAME in the samples was calculated using Eq.3 below as:

$$C = \frac{\sum A - A_{is}}{A_{is}} \times \frac{C_{is} \times V_{is}}{m} \times 100\% \quad 3$$

Where:

$\sum A$  = total peak area of methyl ester

$A_{is}$  = peak area of internal standard (methyl heptadecanoate)

$C_{is}$  = concentration of the internal standard solution, in (mg/ml)

$V_{is}$  = volume of the internal standard solution used, in (ml)

$m$  = mass of the sample, in (mg).

### Determination of Biodiesel Properties

The properties of the biodiesel were set on using ASTM 6751D method. The properties determined include specific gravity, kinematic viscosity and acid value using Eq.5 (Mohibbe et al., 2005), Cetane number (CN) and higher heating value (HHV) were estimated from Eq. 4 (Muhammad et al., 2017), while the iodine value (IV) and saponification value were determined from the Eq.6 and Eq.7 respectively.

$$\frac{N \times (V_b - V_s) \times 1000}{W} \left( \frac{\text{Meq}}{\text{kg}} \right) \quad 4$$

Where:

$N$  = Molarity of thiosulphate

$TS$  = volume of thiosulphate used in the sample test.

$TB$  = volume of thiosulphate used in the blank.

$W$  = Weight of oil Sample.

$$SV = \frac{(V_b - V_s) \times 56.1 \times M}{\text{wt of biodiesel}} \quad 5$$

Where:

$b$  = volume in cm<sup>3</sup> of 0.1M HCl required for blank titration

$a$  = Volume in cm<sup>3</sup> of 0.1 M HCl required for sample titration.

$M$  = Molar concentration of HCl

$$IV = \frac{(V_b - V_a) \times M \times 126.9}{W} \quad 6$$

Where:

126.9 = Atomic weight of iodine,

$M$  = molarity of Na<sub>2</sub>S<sub>2</sub>O<sub>3</sub>·5H<sub>2</sub>O solution,

$W$  = weight of biodiesel sample and

$V_a$  = Titre values for test

$V_b$  = Titre values for blank.

$$CN = 46.3 + \frac{5458}{SV} - 0.225 \times IV - -Eq.7$$

Where: CN= cetane Number.

IV= Iodine Value.

SV= Saponification Value., PV= Peroxide value.

RESULTS AND DISCUSSION

Catalyst characterization

FT-IR

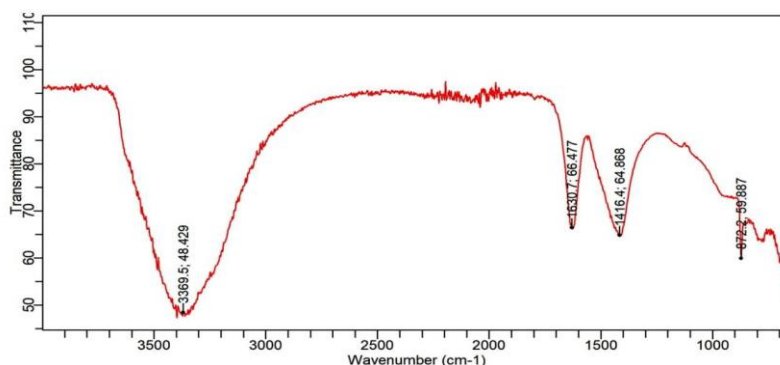


Figure 1: FT-IR Spectra of the Catalyst

The spectra shows an intensive broad vibration bands in the region 3369.5 cm<sup>-1</sup> attributed to OH-group stretching vibrations of OH groups due to water on the solid catalyst (Li and Rudolph, 2008). The existence of hydroxyl group absorption resulted from absorption of atmospheric moisture during FT-IR analysis, which subsequently formed metallic hydroxide. This phenomenon was common due to the high hydrophilicity nature of the catalyst (Tan et al., 2015). The weak peaks at 875cm<sup>-1</sup> correlate with the out-of-plane bending vibration of C-O bonds of carbonates. The reduced intensity of absorption band seen at, 1630.7 cm<sup>-1</sup> and 1416.4 cm<sup>-1</sup> can be attributed to Metallic oxides from carbide slag

(Galv'an-Ruiz et al., 2009). These groups are probably considered as the active basic sites of the CS-AICl<sub>3(aq)</sub> catalyst. These outcomes are in good agreement with that reported by (Cherikkallinmel et al., 2015; Marinkovic, et al., 2016).

XRD of Analysis of the Catalyst (CS-AICl<sub>3(aq)</sub>)

The XRD pattern (Figure1) revealed the crystalline phase of the material as cellulose, Bornite and periclase with well-defined diffraction peaks at 2θ°.The table.1 and 2 below shows the values obtained from the XRD analysis; while Figure 1. Shows the X-ray diffraction patterns.

Table 1: X-ray diffraction patterns of Peaks

2θ°	dÅ	Phase Name	Chemical Formular
239(59123)	4(14...	Cellulose Iβ:0	C <sub>12</sub> H <sub>14</sub> D <sub>10</sub> O <sub>6</sub>
47.89(2)	1.8995(8)	Cellulose Iβ:4	C <sub>12</sub> H <sub>14</sub> D <sub>10</sub> O <sub>6</sub>
79.05(8)	1.2114(1..	Bornite:15	Cu <sub>1.375</sub> Fe <sub>0.275</sub> S
86(1169104)	1.1(17)	Cellulose Iβ:0	C <sub>12</sub> H <sub>14</sub> D <sub>10</sub> O <sub>6</sub>

Table 2: Qualitative Analysis Result

Phase Name	Chemical Formula	FOM
Cellulose	C <sub>12</sub> H <sub>14</sub> D <sub>10</sub> O <sub>6</sub>	0.887
Bornite	Cu <sub>1.375</sub> Fe <sub>0.275</sub> S	3.214
periclase	MgO	0.597

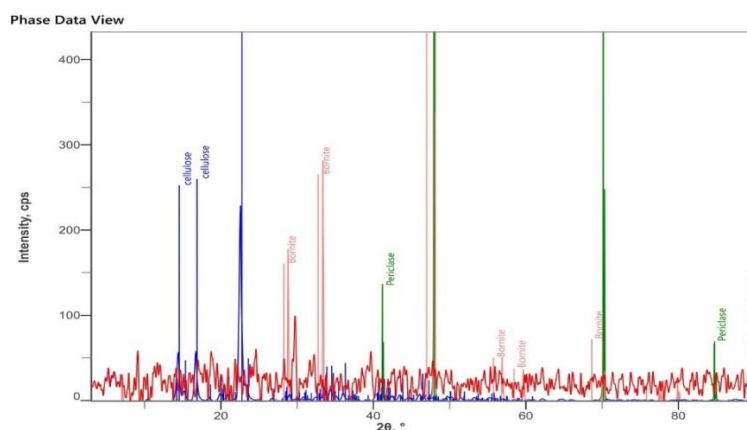


Figure 1: XRD pattern of Catalyst (CS-AICl<sub>3(aq)</sub>)

**SEM Analysis**

The structural morphologies of supports carbide slag and crude Aluminium chloride prepared by digesting waste Aluminium foil in conc. HCl (aq). In general, the images show randomly distribution of different particles size with varying

geometries, which cluster to form an irregular morphology plates for the catalyst. The smaller dimensions of the grains and cluster of carbide slag could provide a higher specific surface area (Buasri et al., 2013). Figure.2. below shows SEM of the heterogeneous catalyst.

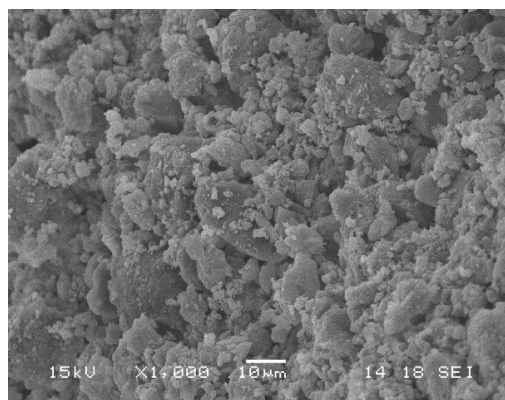


Figure 2: SEM Image of the Catalyst (CS-AlCl<sub>3</sub> (aq))

**Design of Experiment**

**Table 3: Variables in *In-situ* Transesterification and their Levels used in Box-Behnken Design**

Independent Variables	Coding	Lower level	Upper level
Temperature, (°C)	$\theta$	40.0	60.0
Time, (hr)	$t$	1.00	3.00
Methanol, (cm <sup>3</sup> )	$m$	40.0	60.0

**Analysis of variance table**

**Table 4: Result of Analysis of Variance for castor seed biodiesel (CSB) Yield %**

Source	Code	DF	Adj SS	Adj MS	F-Value	P-Value
<b>Model</b>		15	1151.82	76.788	10.98	0
<b>Blocks</b>		1	72.22	72.221	10.33	0.005
<b>Linear</b>		4	524.35	131.088	18.75	0
<b>Temp.(°C)</b>	( $\theta$ )	1	50.55	50.553	7.23	0.015
<b>Time (hr)</b>	( $t$ )	1	18.74	18.745	2.68	0.119
<b>Vol. Methanol (cm<sup>3</sup>)</b>	( $m$ )	1	408.54	408.544	58.44	0
<b>Weight of Cat (g)</b>	( $w$ )	1	47.77	47.768	6.83	0.018
<b>Square</b>	S <sup>2</sup>	4	458.09	114.522	16.38	0
<b>Temp. (°C)*Temp. (°C)</b>	( $\theta^2$ )	1	271.41	271.408	38.82	0
<b>Time (hr)*Time (hr)</b>	( $t^2$ )	1	93.46	93.464	13.37	0.002
<b>Methanol(cm<sup>3</sup>)*Methanol(cm<sup>3</sup>)</b>	( $m^2$ )	1	34.81	34.815	4.98	0.039
<b>Wt. of Cat (g)*Wt. of Cat (g)</b>	( $w$ )	1	51.45	51.445	7.36	0.014
<b>2-Way Interaction</b>		6	317.82	52.969	7.58	0
<b>Temp(°C)*Time (hr)</b>	( $\theta*t$ )	1	22.63	22.634	3.24	0.089
<b>Temp(°C)*Methanol(cm<sup>3</sup>)</b>	( $\theta*m$ )	1	79.38	79.38	11.35	0.003
<b>Temp(°C)*Wt. of Cat (g)</b>	( $\theta*w$ )	1	3.97	3.968	0.57	0.461
<b>Time(hr)*Methanol(cm<sup>3</sup>)</b>	( $t*m$ )	1	137.62	137.62	19.69	0
<b>Time(hr)*Wt. of Cat (g)</b>	( $t*w$ )	1	15.05	15.051	2.15	0.16
<b>Methanol(cm<sup>3</sup>)*Wt. of Cat (g)</b>	( $m*w$ )	1	83.39	83.391	11.93	0.003
<b>Error</b>		18	125.84	6.991		
<b>Lack-of-Fit</b>		15	119.33	7.955	3.67	0.156
<b>Total</b>		33	1277.65			

R<sup>2</sup> = 90.15%

R<sup>2</sup>(adj) = 81.74%,

**Key**

DF= degree of freedom. Seq SS = Sequential Sum of Squares. Adj SS= Adjusted Sum of Squares. Adj MS= adjusted mean Squares. F= f-Statistic . P= p-value.

The analysis of variance reveals that the linear, quadratic and interaction terms of the model are statistically significant ( $p < 0.05$ , at  $\alpha = 0.05$ ). The higher coefficient of determination ( $R^2$ ) for castor nut biodiesel (90.15%) shows that the model solemnly describe the observed relationship between the CSB yields and the process variables. all other linear and square terms of the process variables are statistically significant ( $p < 0.05$ ). Thus on eliminating the insignificant terms from the model, the new regression model (Eq. 9.) has ten significant terms (adjusted  $R^2 = 81.74\%$ ). In general, the empirical model

(Eq.8) serves as a better representation of the *In-situ*-transesterification process with good prediction power.  
 $\% \text{ Yield Of CSB} = 175.0 - 7.71 (\theta) + 2.44 (m) - 53.3 (w) + 0.0668 (t^2) + 4.18 (t) - 0.0240$

$$(m^2) + 10.71 (w) + 0.03150 (\theta)*(m) - 0.938 (t)*(m) + 0.835 (m)*(w).----- \text{Eq. 9}$$

Figure 2 and 3 shows contour and surface plots describing the relationship between one of the reaction variables while holding the other two variables at constant as they affect the biodiesel yield of Castor bean seed.

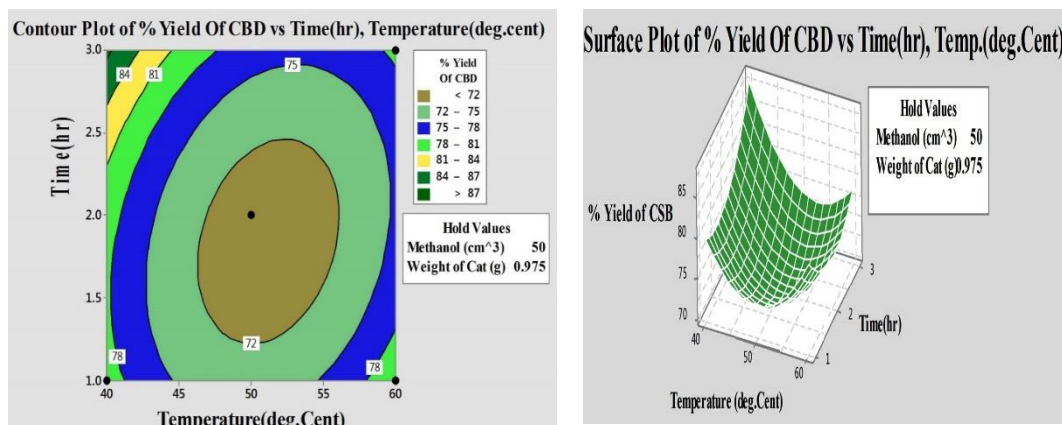


Figure 2: Effect of temperature and reaction time on CSB yield.

The combined effect of reaction time and temperature (Figure 2) prove that biodiesel yield increased with increasing reaction time and temperature. At a higher reaction time and lower temperature ( $< 2.5\text{hr}$ ,  $\leq 40^\circ\text{C}$ ), the biodiesel yield was

84% due to fact oil produced from the castor bean has low viscosity in consequence the *in-situ* transesterification can be performed at room temperature (Bueno et al., 2017; Bateni et al., 2018).

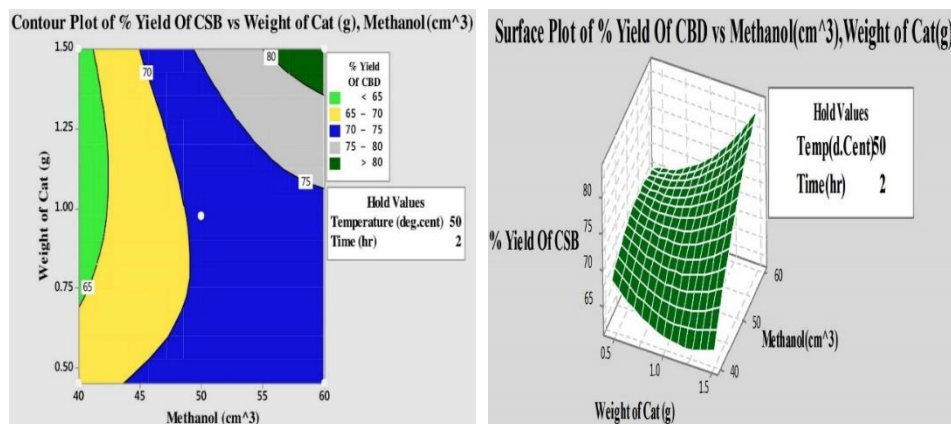


Figure 3: Effect of Volume of methanol and weight of catalyst on biodiesel yield

Figure 3. Shows that the volume of methanol and weight of catalyst also interact positively to influence the biodiesel yields of the castor seed. When volume of methanol was  $40\text{cm}^3$  at maximum catalyst loading of  $0.75\text{g}$  the yield of

biodiesel achieved was 65% .Maximum yield of biodiesel ( $> 80\%$ ) are obtained when the *in-situ* transesterification of castor seed was conducted under  $55\text{cm}^3$  to  $60\text{cm}^3$  volume of methanol and  $1.5\text{g}$  of catalyst loading.

Table 5: Result of optimization of castor seed biodiesel (CSB)

Solution	Temp.(°C)	Time(hr)	Methanol( $\text{cm}^3$ )	Wt of Cat(g)	% Yield Of CBD	Desirability
1	40	1	60	1.5	97.68	1
2	40	3	40	1.5	95.81	1
3	60	1	60	0.45	95.72	1
<b>Global</b>	<b>40</b>	<b>1</b>	<b>60</b>	<b>1.5</b>	<b>97.68</b>	<b>1</b>

The result above implies that the most optimal solution is solution 1 with catalyst loading (1.5g) and 60cm<sup>3</sup> of methanol which result to a yield of 97.68% while the further increase in reaction time of 3hrs in (solution 2) leads to decrease in the percentage yield of biodiesel. The global solution (solution 1) which required temperature, Volume of methanol, weight of catalyst of 60cm<sup>3</sup>, 40 °C, 1hrs and 1.5g respectively may therefore be attractive for *In-situ* transesterification of castor seed oil into FEME via *In-situ* transesterification.

**Biodiesel Characterization**

FT-IR and GC-MS spectrophotometers were used to identify the biodiesel formation. The FT-IR spectra of all biodiesel samples showed a similar pattern. The FT-IR spectrum of biodiesel was different with triglyceride in peak area of 1200 cm<sup>-1</sup>, which is specified of the functional groups of methoxy (-OCH<sub>3</sub>) as shown in Figure 4.

**FT-IR Analysis**

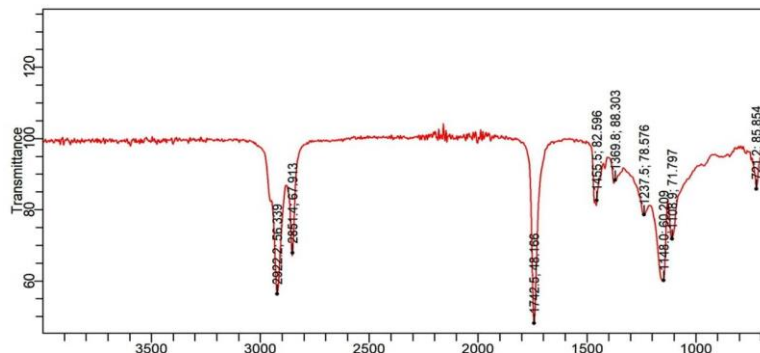


Figure 4: FT-IR Spectra of Biodiesel Sample from *Ricinus Communis* (Castor bean nut)

**GC-MS Analysis**

The GC-MS profile of the castor nut fatty acid methyl esters is dominated by; Methyl-12-hydroxy-9-Cis-Octadecenoate, Cis-Methyl 9-12-Octadecadienoate, Cis-Methyl 9-

Octadecenoate, and Methyl hexadecanoate ester are discovered in the biodiesel sample. From Table: 5 above below 96.20% biodiesel conversion was achieved using the catalyst.

**Table 6: GC-MS Fatty Acid Methyl Ester Compositions of Castor Bean Seed Biodiesel (CSB)**

Systematic Name	Formular	Retention time	Peak Area (%)	% of CSB
Methyl hexadecanoate	C <sub>17</sub> H <sub>34</sub> O <sub>2</sub>	18.56	4212415.261	2.034
Cis-Methyl-9-hexadecenoate	C <sub>17</sub> H <sub>32</sub> O <sub>2</sub>	16.86	3000295.089	0.145
Methyl Octadecanoate	C <sub>19</sub> H <sub>38</sub> O <sub>2</sub>	20.57	2143485.642	1.035
Cis-Methyl 9-Octadecenoate	C <sub>19</sub> H <sub>36</sub> O <sub>2</sub>	21.96	6353829.902	3.068
Cis-Methyl 9-12-Octadecadienoate	C <sub>19</sub> H <sub>34</sub> O <sub>2</sub>	20.69	9597016.873	4.634
Cis-Methyl 6-9-12-Octadecatrienoate	C <sub>19</sub> H <sub>32</sub> O <sub>2</sub>	18.12	896743.2685	0.433
Methyl-12-hydroxy-9-Cis-Octadecenoate	C <sub>19</sub> H <sub>36</sub> O <sub>3</sub>	21.68	175730615.6	84.853

**Table 7: Physicochemical Properties of Biodiesel**

PROPERTIES	CSB FAME	ASTM D6751-06a
Acid value (mg KOH/g)	0.64 ± 0.18	≤ 0.5 max
Saponification value (mg KOH/g)	176.02 ± 0.18	—
Kinematic viscosity @ 40°C (mm <sup>2</sup> /s)	15.67 ± 0.00	1.90 – 6.00
Cetane Number (min)	40.33 ± 0.00	≥ 51min
Iodine Value (gI <sub>2</sub> /100 g)	82.45 ± 0.15	nd
Flash Point (°C)	172 ± 0.00	≤ 130max
Pour Point (°C)	-32 ± 0.00	-15 – -10

Values are means ± SD triplicates analysis of the sample

The Physicochemical Properties of CSB FEME reveal that the saponification value obtains is in line with the previous literatures similarly; (176.02 mg KOH/g of oil) by (Molefe et al., 2017) and (Kaur and Bhaskar, 2019), Saponification value below 190 mg/KOH is an indication that high molecular weight fatty acids are present in biodiesel (Onyema et al., 2014). Kinematic viscosity@ 40°C (15.67 mm<sup>2</sup>/s) is in line with previous literatures of (Molefe et al., 2017; Damlami et al., 2015) but different from result obtained by (Ramachandran et al., 2011; Kaur and Bhaskar, 2019). The maximum acceptable limit of viscosity according to ASTM

D6751 ranges are (1.9–6.0mm<sup>2</sup>/s) (Yusuf et al., 2011). The cetane number reported (61.33 min) were in line with the earlier literatures of (Molefe et al., 2017; Ramachandran et al., 2011). Cetane number (CN) obtained was in order with that obtained by (Molefe et al., 2017) even so exceeding that obtained (Ramachandran et al., 2011). CN increases with increasing length of both fatty acid chain and ester groups (Knothe, 2005). CN of diesel specified by ASTM D6751 is 51 min (Lapuerta et al., 2008). The lower CN result in Low acid value High flashpoint of the CSB FAME (Bueno et al., 2017; Bateni et al., 2018).

## CONCLUSIONS

Biodiesel production around the world results from different feedstocks and specifically vegetable oils. Besides, there exist a wide heterogeneity of methods to obtain biofuels; however, the most economical is *In-situ* transesterification, which detach the purification steps in the biodiesel production steps. The empirical experimental model obtained expresses the relationship between the biodiesel and the statistical significant reaction variables at ( $R^2 = 90.15\%$ ). The conversion of 97.68% was achieved under the optimum reaction conditions of 1.5g. wt of CS-AlCl<sub>(aq)</sub>, (1:9) of seed to methanol ratio, 1hrs of reaction time and 40°C of temperature which correlate with 96.20% total fatty acid methyl ester composition reveal by GC-MS result. The biodiesel produced were characterized using FTIR and GC-MS. The physicochemical properties of the biodiesel produced was compared with the standards specified by (ASTM). The Biodiesel from castor oil offers environmental and technical benefits, therefore, it can be considered as a viable alternative in the present and future to other forms of biodiesel. Moreover, the feedstock can replace 40–50% of edible oil currently used in biodiesel production. Furthermore, the Ricinoleic fatty acid offers advantages to the *In-situ* transesterification process such as high miscibility in alcohol low reaction temperature, low iodine content and low freezing point. Reprocess of carbide slag and waste aluminium foil into more useful and environmental friendly catalyst can bring down the rate of pollution. Finally, the union of these three will give rise to low cost and competitive potential biodiesel in comparison with petrodiesel.

## ACKNOWLEDGMENTS

The authors thank Central Advance Science laboratory Complex (CaSLac) for the support provided.

## CONFLICT OF INTEREST

The authors declare no conflict of interest.

## REFERENCES

AOAC (1990): Official Method of Analysis 15<sup>th</sup> Edition, Association of official Analytical Chemist, Washington DC.

Aranda-Rickert, A., Morzán, L., Fracchia, S. (2011): Seed oil content and fatty acid profiles of five Euphorbiaceae species from arid regions in Argentina with potential as biodiesel source. *Journal of Seed Sciences Research*. **21**: 63–68.

ASTM, (6751D) American Standard for Testing of Materials, (2008): Characteristics of *Jatropha Curcas* Oil. *Journal of American Oil and Chemist Society*, **85**: 2671–2678.

Batani, H., Saraeian, A., Able, C. and Karimi, K. (2018): Biodiesel Purification and Upgrading Technologies. *Biofuel and Biorefinery Technologies*, 57-100

Bauidh, K., Singh, K., Singh, B., Singh, R.P. (2015): *Ricinus communis*: A robust plant for bio-energy and phytoremediation of toxic metals from contaminated soil. *Journal Ecological Engineering*. **84**: 640–652.

Buasri, A., Chaiyut, N., Loryuenyong, V., Worawanitchaphong, P. and Trongyong, S. (2013): "Calcium oxide derived from waste shells of mussel, cockle, and scallop as the heterogeneous catalyst for biodiesel production," *The Scientific World Journal*, **1**:1-7.

Bueno, A.V., Pereira, M.P.B., de Oliveira Pontes, J.V., de Luna, F.M.T. and Cavalcante, C.L. (2017): Performance and emissions characteristics of castor oil biodiesel fuel blends. *Applied Thermal Engineering*, **125**: 559-566.

Cherikkallinmel, S., Gopalakrishnan, A., Yaakob, Z., Ramakrishnan, R., Sugunan, S., and Binitha, N. (2015): Sodium Aluminate from Waste Aluminium Source as Catalyst for the Transesterification of *Jatropha* Oil. *Royal Society of Chemistry Advances*, **5**:46290.

Danlami, J.M., Agus, A. and Muhammad, A.A.Z. (2015): Characterization and process optimization of castor oil (*Ricinus communis L.*) extracted by the soxhlet method using polar and non-polar solvents. *Journal of the Taiwan Institute of Chemical Engineers*, **47**: 99-104.

Ehimen, E.A., Sun, Z.F. and Carrington, C.G. (2010): "Variables Affecting The *In-Situ* Transesterification Of Microalgae Lipids", *Fuel*, **89**(3): 677-684.

Galadima, A. and Muraza, O. (2020): Waste materials for production of biodiesel catalysts: Technological status and prospects, *Journal of Cleaner Production*, (263): 121-125.

Galv'an-Ruiz, M., Hern'andez, J., Bayos, L., Noriega-Montes, J., Mario, E. and Rodr'iguez, G. (2009): "Characterization of calcium carbonate, calcium oxide, and calcium hydroxide as starting point to the improvement of lime for their use in construction, *Journal of Materials in Civil Engineering*, **21**(11): 694–698.

Keera., S.T. Sabagh., S.M.E. Taman., A.R. (2018): Castor oil biodiesel production and optimization. *Egyptian Journal of Petroleum*. **27**: 979–984.

Knothe, G. (2005): Dependence of Biodiesel Fuel Properties on the Structure of Fatty Acid Alkyl Esters, *Fuel Process Technology*. **88**:1059-1070

Kumar, D., Das, T., Giri, B.S. and Verma, B. (2020): Preparation and characterization of novel hybrid bio-support material immobilized from *Pseudomonas cepacia* lipase and its application to enhance biodiesel production. *Renew. Energy*, **147**: 11–24.

Lapuerta, M., Armas, O. and Rodriguez-Fernandez, J. (2008): Effect of Biodiesel Fuels on Diesel Engine Emissions. *Progressive Energy Combustion Science*. **34**(2):198–223.

Li, E. and Rudolph, V. (2008): Transesterification of Vegetable Oil to Biodiesel over Mgo Functionalized Mesoporous Catalysts, *Energy Fuel*. **22**: 145–149.

Marinkovic, M. M., Stojkovic, N. I., Vasic, M.B., Ljupkovic, R. B., Rancic, S. M., Spalovic, B. R. and Zarubica, A. R. (2016): Synthesis of Biodiesel from Sunflower oil Over Potassium Loaded Alumina as Heterogeneous Catalyst: The Effect of Process Parameters: *Hemijaska Industrija On Line-First*, 1-1.

McKeon, T.A. (2016): Castor (*Ricinus communis L.*) in Industrial Oil Crops; *Elsevier: Amsterdam, the Netherlands*, 75–112. ISBN 978-1-893997-98-1.

Mohibbe, M.A., Waris, A. and Nahar, N.M. (2005): Prospects and Potential of Fatty acid Methyl Esters of Some Non-

Traditional Seed Oils for Use as Biodiesel in India *Journal of Biomass And Energy*, (29): 293-302

Molefe, M., Diakanua, N. and Hembe, E. M. (2019): Method Selection for Biojet and Biogasoline Fuel Production from Castor Oil: A Review. *Energy & Fuels*, **33**: 5918-5932.

Muhammad, A.B., Obianke, M., Gusau, L.H. and Aliero, A.A. (2017): Optimization of Process Variables in Acid Catalysed *In-Situ* Transesterification of *Hevea Brasiliensis* (Rubber Tree) Seed Oil into Biodiesel. *Biofuels*, **8**: 585-594.  
National Toxicology Program (NTP) (2003): Chemical Repository. Castor oil. Research Triangle Park, NC: 27709, 13-32.

Onyema, C. T., Okerenwogba, F. O., Iloameke, I. M., Ekwueme, I. J., Ejiagha, M. C. and Ohaekenyema, E. C. (2014): Extraction and Characterization of Biodiesel from Cashew Nuts and Shells Oil (*Anacardium Occidentale*). *American Journal of Science and Technology*. **1(5)**: 344-347.

Ramachandran, K., Pandian, S., Tamilarasan, S. and Sahadevan, R. (2011): Production of biodiesel from mixed waste vegetable oil using an aluminium hydrogen sulphate as a heterogeneous acid catalyst. *Bioresource Technology*, **102**: 7289-7293.

Samuel, O., Eng, M., and Dairo, O. (2012): A Critical Review of *In-Situ* Transesterification Process for Biodiesel Production. *The Pacific Journal of Science and Technology*, (72): 72-79.

Tan, Y. H., Abdullah, M. O., Nolasco-Hipolito, C. and Taufiq Yap, Y. H. (2015): "Waste Ostrich and Chicken-Eggshell as heterogeneous base Catalyst for Biodiesel production from used Cooking Oil: Catalyst Characterization and Biodiesel yield Performance, *Applied Energy*, **160**:58-70.

Tarigan, J.B., Prakoso, H.T., Siahaan, D. and J. Kaban, J. (2017): Rapid Biodiesel Production from Palm Kernel through *In-Situ* Transesterification Reaction Using CaO as Catalyst. *International Journal of Applied Chemistry*, **13(3)**: 631-646.

Wotto, D.V., N'dayishimiye, V., Yété, P., Sessou, P., Agbangnan, P. and Sohounhloúé, D. (2015): Physico-Chemical Characterization of Oil and Defatted Meal From *Anacardium Occidentale* Acclimated to Teval in Northern Benin. *World Journal of Pharmacy and Pharmaceutical Sciences*. **4 (11)**: 1912-1920.



©2022 This is an Open Access article distributed under the terms of the Creative Commons Attribution 4.0 International license viewed via <https://creativecommons.org/licenses/by/4.0/> which permits unrestricted use, distribution, and reproduction in any medium, provided the original work is cited appropriately.